# 9

# Electrostatic Precipitators

## 9.1 INTRODUCTION

An electrostatic precipitator (ESP) is a particle control device that uses electrical forces to move the particles out of the flowing gas stream and onto collector electrodes. They range in size from those installed to clean the flue gases from the largest power plants to those used as small household air cleaners. ESPs account for about 95% of all utility particulate controls in the U.S. (Offen and Altman 1991). The particles are given an electrical charge by forcing them to pass through a corona, a region in which gaseous ions flow. The electrical field that forces the charged particles to the walls comes from discharge electrodes maintained at high voltage in the center of the flow lane.

Once the particles are on the collecting electrodes, they must be removed from the surface without reentraining them into the gas stream. This is usually accomplished by knocking them loose from the plates, allowing the collected layer of particles to slide down into a hopper from which they are evacuated. Some ESPs remove the particles by intermittent or continuous washing with water. Precipitators are unique among particulate matter control devices in that the forces of collection act only on the particles and not on the entire gaseous stream. This phenomenon typically results in a high collection efficiency (above 99.5%) with a very low gas pressure drop.

## 9.2 TYPES OF ESPS

**Your objectives in studying this section are to**

1. Identify the most common ESP configurations: (1) plate-wire, (2) flat plate, (3) tubular, (4) wet, and (5) two-stage.
2. Describe the operating characteristics and advantages of each configuration.
3. Understand the importance of reentrainment, gas sneakage, and dust resistivity.

ESPs are configured in several ways. Some of these configurations have been developed for special control actions, while others have evolved for economic reasons. A description of the most common configurations follows.

### 9.2.1 Plate-Wire Precipitators

This configuration is used in a wide variety of industrial applications including coal-fired boilers, cement kilns, solid waste incinerators, paper mill recovery boilers, petroleum refining catalytic cracking units, sinter plants, open hearth furnaces, coke oven batteries, and glass furnaces (Turner et al. 1988 a).

In a plate-wire ESP, gas flows between parallel plates of sheet metal. Weighted high-voltage wire electrodes hang between the plates as shown schematically in Figure 9.1. Within each flow path, the gas must pass each wire sequentially as it flows through the unit.

The plate-wire ESP allows many flow lanes to operate in parallel, and each lane can be quite tall. Therefore, this type of precipitator is well suited for handling large volumes of gas. The need for rapping the plates to dislodge the collected material causes the plates to be divided into sections, often three or four in series, which can be rapped independently. The power supplies are usually sectionalized in the same manner to obtain higher operating voltages.

The power supplies for the ESP convert the industrial AC voltage (220–440 V) to pulsating DC voltage in the range of 20 to 100 kV as needed. The voltage applied to the electrodes causes the gas between the plates to break down electrically, an action known as a "corona." The electrodes usually are given a negative polarity because a negative corona supports a higher voltage than a positive corona before sparking occurs. The ions generated in the corona follow electric field lines from the wires to the collecting plates. Therefore, each wire establishes a charging zone through which the particles must pass.

Particles passing through the charging zone absorb some of the ions. Small aerosol particles (less than 1-μm diameter) can absorb tens of ions before their total charge becomes large enough to repel further ions. Large particles (more than 10-μm diameter) can absorb tens of thousands of ions. The electrical forces are therefore much stronger on the large particles.

As the particles pass each successive wire, they are driven closer and closer to the collecting walls. The turbulence in the gas, however, tends to keep them uniformly mixed with the gas. The collection process is a competition between the electrical and dispersive forces. Eventually the particles approach close enough to the walls so that the turbulence drops to low levels and the particles are collected.

Reentrainment of the particles during rapping reduces the efficiency of the ESP. The rapping that dislodges the accumulated dust also projects some of the particles (typically 12% for coal fly-ash) back into the gas stream. These reentrained particles are then processed again by later sections, but the particles reentrained in the last section of the ESP have no chance to be recaptured and so escape the unit. Part of the gas flows around the charging zone into the space provided to support and align the electrodes. This is called "sneakage" and amounts to 5% to 10% of the total flow. Antisneakage baffles force the sneakage flow to mix with the main gas stream

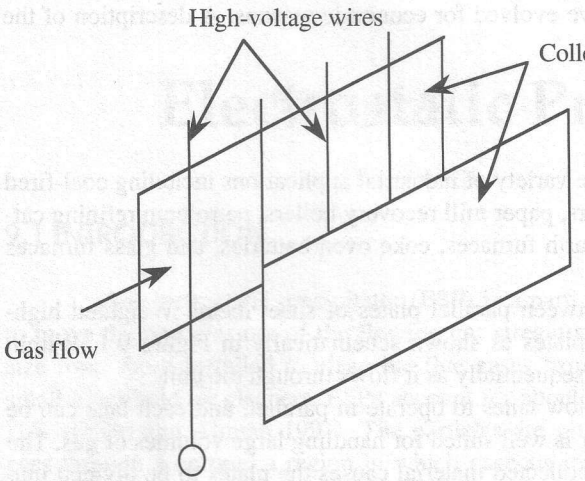


**Figure 9.1** Schematic diagram of a plate-wire ESP

for collection in later sections. But, again, the sneakage flow around the last section has no opportunity to be collected.

Another major factor that affects the performance of ESPs is the resistivity of the collected material. Because the particles form a continuous layer on the ESP plates, all the ion current must pass through the layer to reach the ground plates. This creates an electric field in the layer which can become large enough to cause local electrical breakdown called "back corona." Back corona is prevalent when the resistivity of the layer is high, usually above $2 \times 10^{11}$ ohm-cm. It reduces the collection ability of the unit because severe back corona causes difficulty in charging the particles. Conversely, at resistivities below $10^8$ ohm-cm, the particles hold on to the plates so loosely that reentrainment becomes much worse. The resistivity is strongly affected by temperature, moisture, gas composition, particle composition, and surface characteristics.

### 9.2.2 Flat Plate Precipitators

A significant number of smaller ESPs (50–100 $m^3/s$) use flat plates instead of wires for the high-voltage electrodes. The flat plates increase the average electric field and the surface area available for the collection of particles. Flat plates can not generate corona by themselves, so corona generating electrodes are placed ahead of and sometimes after the discharge plate zone. These electrodes may be sharp-pointed needles attached to the edges of the plates or independent corona wires. Unlike plate-wire or tubular ESPs, this design operates equally well with either positive or negative polarity. A positive polarity reduces ozone generation.

A flat plate ESP operates with little or no corona current flowing through the collected dust, except directly under the corona needles or wires. This makes the unit less susceptible to back corona than conventional precipitators. However, the lack of current in the collected layer

causes an electrical force that tends to dislodge the layer from the collecting electrode leading to high reentrainment losses during rapping. The dislodging electrical force is stronger for large particles.

Flat plate ESPs have wide application for high-resistivity particles with small MMDs (1–2 μm). Fly-ash has been successfully collected with this type of precipitator, but low-flow velocity appears to be critical for avoiding high rapping losses.

### 9.2.3 Tubular Precipitators

The original ESPs were tubular, with the high-voltage wire running along the axis of the tube. Today they comprise only a small portion of the precipitator population and are most commonly applied where the particulate is either wet or sticky—for example, in sulfuric acid plants. There are no sneakage paths and, because they are usually cleaned with water, reentrainment losses are much lower.

### 9.2.4 Wet Precipitators

Any of the precipitator configurations described earlier may be operated with wet walls. The water flow may be applied intermittently or continuously to wash the collected particles into a sump for disposal. This type of ESPs has no problems with rapping reentrainment or with back corona. The wash increases the complexity of the device, and the collected slurry must be handled more carefully than a dry product adding to the expense of final disposal.

### 9.2.5 Two-Stage Precipitators

This configuration separates particle charging and collecting functions to optimize the electrical conditions for each. Charging requires a high current density and electric field, whereas collection requires high electrical fields but much less current. The two-stage ESP is a series device with the discharge electrode, or ionizer, preceding the collector electrodes. Advantages for this configuration include more time for particle charging, less propensity for back corona with high-resistivity ash, and economical construction for small sizes.

This type of precipitator is usually applied for gas flow rates of 25 $m^3/s$ or less. The smaller devices are often sold as preengineered package systems consisting of a mechanical prefilter, ionizer, collecting-plate cell, after-filter, and power pack. Recent work suggests that the addition of a precharger to a conventional precipitator is an economical way to convert it from single- to two-stage operation when handling high-resistivity ash (Offen and Altman 1991).

## 9.3 ELECTROSTATIC PRECIPITATION THEORY

**Your objectives in studying this section are to**

1. Develop the grade-efficiency equation for an ESP.
2. Estimate the average operating electric field strength for an ESP.
3. Estimate the total charge on a particle by diffusion and field charging.
4. Estimate grade efficiencies of an ESP with Feldman's model.

The theory of ESP operation requires many scientific disciplines to describe it thoroughly. The ESP is basically an electrical machine. The principal actions are the charging of particles and forcing them to the collector plates. The transport of the particles is affected by the level of turbulence in the gas. The particle properties also have a major effect on the operation of the ESP.

### 9.3.1 Particle collection

The electric field in the collecting zone produces a force on a particle proportional to the magnitude of the field and to the particle charge:

$$F_e = q_p E_c \tag{9.1}$$

where

$F_e$ = force due to the electric field, newtons (N)

$q_p$ = charge on the particle, coulombs (C)

$E_c$ = strength of the electric field in the collecting zone, volt/meter (V/m)

The motion of the particles under the influence of the electric field is opposed by the viscous drag force of the gas. When the drag force exactly balances the electrostatic force, the particle attains its terminal velocity, $u_t$. Assuming that the particle obeys Stokes's law,

$$u_t = \frac{q_p E_c C_c}{3\pi\mu D_p} \tag{9.2}$$

where

$C_c$ = Cunningham correction factor

$D_p$ = particle diameter

## Example 9.1 Terminal Velocity Of Charged Particle In Electric Field

Dust particles of 1.0-μm diameter with an electric charge of $3 \times 10^{-16}$ C and a density of 1,000 kg/m$^3$ come under the influence of an electric field with a strength of 100,000 V/m. The particles are suspended in air at 298 K and 1 atm.
(a) Estimate the terminal velocity of the particles.
(b) Calculate the ratio of the electrostatic force to the force of gravity on the particle.

### Solution

(a) For 1.0-μm diameter particles in air at 298 K and 1 atm, the Cunningham correction factor is $C_c = 1.168$. From Eq. (9.2), $u_t = (3 \times 10^{-16})\,(10^5)\,(1.168)/[(3\pi)(1.84 \times 10^{-5})(10^{-6})] = 0.202$ m/s

(b) The ratio of electrostatic to gravity force acting on the particle is:

$$\frac{F_e}{F_g} = \frac{6q_pE_c}{\pi\rho_p g D_p^3} = \frac{(6)\left(3 \times 10^{-16}\right)\left(10^5\right)}{\pi\,(1000)(9.8)\left(10^{-18}\right)} = 5{,}847$$

---

Equation (9.2) gives the particle velocity with respect to still air. In the ESP, the flow is usually very turbulent, with instantaneous gas velocities of the same magnitude as the particles' terminal velocity, but in random directions. The eddying motion owing to turbulence causes a uniform distribution of particles through most of the flow passage. The capture zone is limited to the laminar boundary layer in the vicinity of the collecting electrode. The physical situation is similar to that of turbulent-flow settling chambers (see Problem 7.13). The resulting grade efficiency equation is

$$\eta(D_p) = 1 - \exp\left[-\frac{A_c u_t}{Q}\right] \tag{9.3}$$

where

$A_c$ = total collecting electrode area
$Q$ = gas volumetric flow rate

## Example 9.2 Collection Efficiency of Tubular ESP

Assume that the conditions of Example 9.1 correspond to a tubular ESP with a diameter of the collecting electrode of 2.9 m and a length of 5.0 m. If the gas flow rate is 2.0 $m^3/s$, estimate the collection efficiency for 1.0-μm diameter particles. Corroborate the assumptions of turbulent flow and Stokes's law applicability.

### Solution

Figure 9.2 shows schematically the tubular precipitator arrangement. Assuming turbulent flow, Eq. (9.3) gives the grade efficiency. The collection area for a tubular precipitator is the area of the curved surface, $A_c = \pi DL = \pi(2.9)(5) = 45.55\ m^2$. Therefore, $\eta(1\ \mu m) = 1 - \exp[-(45.55)(0.202)/(2.0)] = 0.99$ (99%).

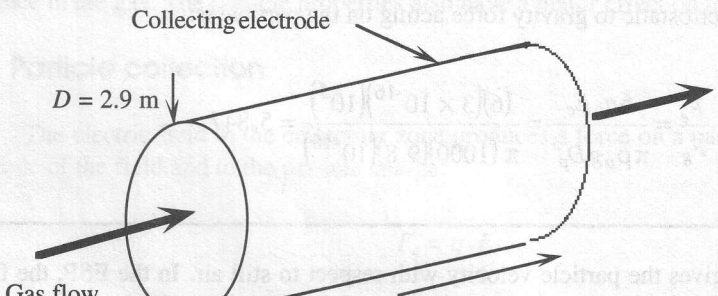


**Figure 9.2** Tubular ESP of Example 9.2

To corroborate the assumption of turbulent flow, calculate the Reynolds number for the gas flow through the circular conduit, $Re = \rho vD/\mu$, where $v$ is the average gas velocity. For the given conditions, $v = (4)(2)/[\pi(2.9)^2] = 0.3$ m/s. The Reynolds number is $Re = (1.185)(0.303)(2.9)/(1.84 \times 10^{-5}) = 56{,}600$. Therefore, the gas flow is fully turbulent.

To corroborate the applicability of Stokes's law, calculate the terminal Reynolds number for the particles, $Re_p = \rho u_t D_p/\mu = (1.185)(0.202)(10^{-6})/(1.84 \times 10^{-5}) = 0.013$. Therefore, Stokes's law applies.

### 9.3.2 Electrical operating point

The electrical operating point of an ESP section is the value of voltage and current at which the section operates. The best collection occurs when the highest electric field is present, which roughly corresponds to the highest voltage on the electrodes. The term section represents one set of plates and electrodes having a common power source.

The lowest acceptable voltage is the voltage required for the formation of a corona. The negative corona is formed when an occasional free electron near the high-voltage electrode, produced by a cosmic ray, gains enough energy from the electric field to ionize the gas and produce more free electrons. The electric field for which this process is self-sustained has been determined experimentally. For round wires, the field at the surface of the wire is given by White (1963) as

$$E_0 = 3 \times 10^6 f \left[ s.g. + 0.03\sqrt{s.g./r_w} \right] \tag{9.4}$$

where

$E_0$ = corona onset field at the wire surface, V/m

$s.g.$= specific gravity of the gas, relative to air at 293 K and 1 atm

$r_w$ = radius of the wire, m

$f$ = roughness factor

For a clean smooth wire, $f = 1.0$; for practical applications, $f = 0.6$ is a reasonable value (Flagan and Seinfeld 1988).

The voltage that must be applied to the wire to obtain this value of field is found by integrating the electric field from the wire to the collecting electrode. In cylindrical geometry, the field is inversely proportional to the radial distance. This leads to a logarithmic dependence of voltage on electrode dimensions. In the plate-wire geometry, the field spatial variation is more complex, but the voltage still exhibits the logarithmic dependence. The corona onset voltage, $V_0$, is given by

$$V_0 = E_0 r_w \ln\left(\frac{d}{r_w}\right) \tag{9.5}$$

where

$d$ = outer cylinder radius in a tubular ESP

$d = (4/\pi)W$ for plate-wire ESP

$W$ = wire-plate separation

---

## Example 9.3 Corona Onset Voltage in Plate-Wire ESP

A plate-wire ESP handles air at 400 K and 110 kPa. The plate spacing is 300 mm, and the diameter of the discharge wires is 4 mm. Estimate the corona onset voltage.

### Solution

Equation (9.4) gives the corona onset field at the wire surface. The specific gravity of the gas is $s.g. = PT_{ref}/P_{ref}T = (110)(293)/[(400)(101.3)] = 0.795$. Therefore, $E_0 = (3 \times 10^6)(0.6)[0.795 + 0.03\ (0.795/0.002)0.5] = 2.51 \times 10^6$ V/m. Calculate $d = 4W/\pi = 4(150)/\pi = 191$ mm. Equation (9.5) gives the corona onset voltage, $V_0 = (2.51 \times 10^6)(0.002)\ \ln\ (191/2) =$ 22,900 V.

---

The electric field is strongest along the line from wire to plate and is approximated very well, except near the wire, by

$$E_{max} = \frac{V}{W} \tag{9.6}$$

where $V$ = applied voltage. The electric field is not uniform along the direction of gas flow. Turner et al. (1988 a) suggest that the average field for an ESP section is given by

$$E_{av} = \frac{E_{max}}{K} \tag{9.7}$$

where $K$ is a constant which depends on the ESP configuration and the presence of back corona. Table 9.1 gives values of $K$ for some common situations.

**Table 9.1 Ratio of Maximum to Average Eectric Fields in ESPs**

| Configuration | Back corona | $K$ |
|---|---|---|
| Plate-wire | No[a] | 1.75 |
| Plate-wire | Severe | 2.50 |
| Flat plate | No[a] | 1.26 |
| Flat plate | Severe | 1.80 |

[a] Resistivity of the collected dust less than $2 \times 10^{11}$ ohm-cm.
Source: Turner et al. (1988 a).

When the electric field throughout the gap between the wire and the collecting electrode becomes strong enough, a spark occurs. The voltage cannot be increased beyond this point without severe sparking occurring. A reasonable estimate of the sparking field strength, $E_s$, is given by (Turner et al. 1988 a):

$$E_s = 6.3 \times 10^5 \left(\frac{273P}{T}\right)^{0.8} \tag{9.8}$$

where

$E_s$ = sparking field strength, V/m
$T$ = absolute temperature, K
$P$ = gas pressure, atm
The ESP generally operates near this point. $E_{max}$ is equal to or less than $E_s$.

## Example 9.4 Average Electric Field in a Plate-Wire ESP

Estimate the average electric field and the operating voltage for the ESP of Example 9.3. The resistivity of the collected dust is $10^{11}$ ohm-cm.

### Solution

Equation (9.8) gives $E_s = 630{,}000\ [(273/400)(110/101.3)]^{0.8} = 496{,}000$ V/m. $= E_{max}$.

Because the resistivity of the collected dust is less than $2 \times 10^{11}$ ohm-cm, there is no back corona. From Table 9.1, $K = 1.75$, therefore, $E_{av} = 496{,}000/\ 1.75 = 283{,}400$ V/m. The operating voltage is $V = WE_{max} = (0.15)(496{,}000) = 74.4$ kV.

### 9.3.3 Particle Charging

Charging of particles takes place when ions bombard the surface of a particle. Once an ion is close to a particle, it is tightly bound because of the image charge within the particle.The image charge is a representation of the charge distortion that occurs when a real charge approaches a conducting surface. The distortion is equivalent to a charge of opposite magnitude to the real one, located as far below the surface as the real charge is above it. The motion of the fictitious charge is similar to the motion of an image in a mirror, hence the name. As more ions accumulate on a particle, the total charge tends to prevent further ionic bombardment.

There are two principal charging mechanisms: diffusion charging and field charging. Diffusion charging results from the thermal kinetic energy of the ions overcoming the repulsion of the ions already on the particle. Field charging results when ions follow electric field lines until they terminate on a particle. In general, both mechanisms operate for all sizes of particles. Field charging is the dominant mechanism for particles greater than about 2 μm, whereas diffusion charging dominates for particles smaller than about 0.5 μm.

Diffusion charging produces a logarithmically increasing level of charge on particles given by (White 1963)

$$q_d(t) = \frac{2\pi\varepsilon_0 k T D_p}{e} \ln(1 + t/\tau_d) \tag{9.9}$$

where

$q_d$ = particle charge by diffusion

$\varepsilon_0$ = free space permittivity ($8.845 \times 10^{-12}$ C$^2$/N-m$^2$)

$k$ = Boltzmann's constant ($1.38 \times 10^{-23}$ J/K)

$e$ = electron charge ($1.67 \times 10^{-19}$ C)

$t$ = exposure time

$\tau_d$ = characteristic time for diffusion charging given by

$$\tau_d = \frac{\varepsilon_0 \sqrt{8mk\pi T}}{e^2 N D_p}$$

$N$ = number of ions per unit volume

$m$ = mass of an ion

For typical operating conditions, $N = 2 \times 10^{15}$ ions/m$^3$, $m = 5.3 \times 10^{-26}$ kg (Crawford 1976, Licht 1980).

Diffusion charging never reaches a limit, but it becomes very slow after three characteristic times. For fixed exposure times, the charge on the particle is proportional to its diameter.

---

## Example 9.5 Diffusion Charging

Calculate the charge by diffusion on a 1.0-μm diameter particle as a function of time. The gas is air at 400 K and 1 atm. The ion density is $2 \times 10^{15}$ ions/m$^3$, and the mass of a typical ion is $5.3 \times 10^{-26}$ kg.

## Solution

Calculate the characteristic time for diffusion charging, $\tau_d = (8.85 \times 10^{-12})\,[(8)(5.3 \times 10^{-26})(1.38 \times 10^{-23})(\pi)(400)]^{0.5}/[(1.67 \times 10^{-19})^2(2 \times 10^{15})(10^{-6})] = 1.36 \times 10^{-5}$ s. From Eq. (8.9), $q_d = 3.068 \times 10^{-18} \ln [1 + t/(1.36 \times 10^{-5})]$ C. Figure 9.3 shows the variation with time of the charge acquired by the particle by diffusion.

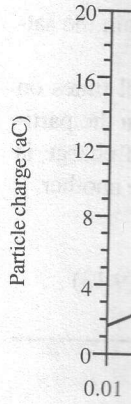


Fi

where

$q_s$ =

$\tau_f$

The saturati

where

$\kappa$ =

$E$ =

The

why field ch

stant is given

where $B$ = io

$10^{-12})/[(2 \times$

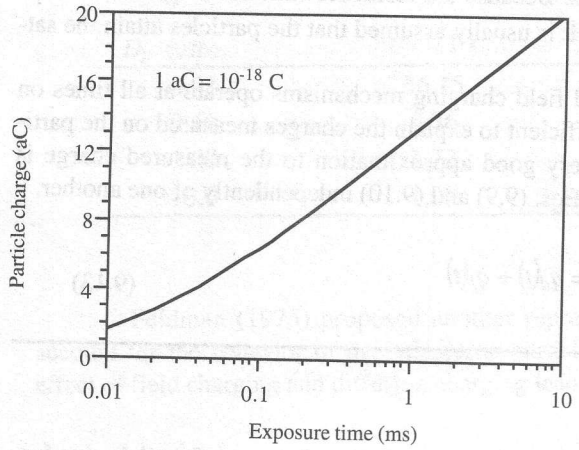


**Figure 9.3** Charging by diffusion of a 1.0-μm diameter particle at 400 K.

Field charging also exhibits a characteristic time-dependence, given by

$$q_f(t) = \frac{q_s t}{t + \tau_f} \tag{9.10}$$

where

$q_s$ = saturation charge (charge at infinite time)

$\tau_f$ = field charging time constant

The saturation charge is given by

$$q_s = \left(\frac{3\kappa}{\kappa + 2}\right) \pi \varepsilon_0 E D_p^2 \tag{9.11}$$

where

$\kappa$ = dielectric constant of the particle

$E$ = external electric field applied to the particle

The saturation charge is proportional to the square of the particle size, which explains why field charging is the dominant mechanism for larger particles. The field charging time constant is given by

$$\tau_f = \frac{4\varepsilon_0}{NeB} \tag{9.12}$$

where $B$ = ion mobility, usually of the order of $10^{-4}$ m$^2$/V-s. For typical conditions, $\tau_f = (4)(8.85 \times 10^{-12})/[(2 \times 10^{15})(1.61 \times 10^{-19})(10^{-4})] = 0.0011$ s. For practical purposes, the saturation charge

may be taken as attained at $t = 100\ \tau_f = 0.1$ s. Because the residence time of the particles in the precipitator generally exceeds a few seconds, it is usually assumed that the particles attain the saturation charge soon after entering the device.

Strictly speaking, both diffusion and field charging mechanisms operate at all times on all the particles, and neither mechanism is sufficient to explain the charges measured on the particles. It has been found empirically that a very good approximation to the measured charge is given by the sum of the charges predicted by Eqs. (9.9) and (9.10) independently of one another.

$$q_p(t) = q_d(t) + q_f(t) \tag{9.13}$$

## Example 9.6 Total Particle Charge

For the following set of conditions, calculate the ratio $q_p/q_s$ as a function of particle size for $t = 0.1$, 1.0, and 10.0 s.

$\kappa = 5.0$ $\quad E = 3 \times 10^5$ V/m $\quad T = 300$ K

$B = 2.2 \times 10^{-4}$ m$^2$/s-V $\quad N = 2 \times 10^{15}$ ions/m$^3$

$m = 5.3 \times 10^{-26}$ kg

### Solution

The field charging time constant is from Eq. (9.12), $\tau_f = 0.000503$ s. Thus, assume that for $t > 0.05$ s the field charging mechanism is saturated. Equation (9.13) becomes

$$q_p = 1.787 \times 10^{-5} D_p^2 + 1.438 \times 10^{-12} D_p \ln\left(1 + 7.79 \times 10^{10} t D_p\right)$$

The first term in this equation is the saturation field charge. Therefore,

$$\frac{q_p}{q_s} = 1 + \frac{8.047 \times 10^{-8}}{D_p} \ln\left(1 + 7.79 \times 10^{10} t D_p\right)$$

where $D_p$ is in meters and $t$ in seconds. The following table presents the ratio $q_p/q_s$ as a function of particle size and exposure time.

| $D_p$ (μm) | $q_p/q_s$ $t = 0.1$ s | $t = 1.0$ s | $t = 10.0$ s |
|---|---|---|---|
| 0.01 | 36.15 | 54.59 | 73.11 |
| 0.10 | 6.36 | 8.21 | 10.06 |
| 1.00 | 1.72 | 1.91 | 2.09 |
| 10.0 | 1.09 | 1.11 | 1.13 |

Feldman (1975) proposed another representation of the total charge on a particle to account for the behavior of the submicron particles. According to Cochet (1961) the combined effect of field charging and diffusion charging leads to:

$$q_p(t) = \left[\left(1 + \frac{2\lambda}{D_p}\right)^2 + \frac{2(\kappa - 1)}{\left(1 + \frac{2\lambda}{D_p}\right)(\kappa + 2)}\right] \pi \varepsilon_0 E D_p^2 \frac{t}{t + \tau_f} \tag{9.14}$$

where $\lambda$ = mean-free path of the gas. For $t >> \tau_f$, Feldman incorporated Eqs. (9.14) and (9.2) into (9.3) to obtain

$$\eta(D_p) = 1 - \exp\left[-\frac{A_c \varepsilon_0 E_c E}{3\mu Q}(C_c F D_p)\right] \tag{9.15}$$

where

$$F = \left[\left(1 + \frac{2\lambda}{D_p}\right)^2 + \frac{2(\kappa - 1)}{\left(1 + \frac{2\lambda}{D_p}\right)(\kappa + 2)}\right] \tag{9.16}$$

In a single-stage precipitator, the electric field in the vicinity of the collecting electrode, $E_c$, and the charging electric field, $E$, are assumed equal to the average field, $E_{av}$. Equation (9.15) becomes

$$\eta(D_p) = 1 - \exp\left[-\frac{A_c \varepsilon_0 E_{av}^2}{3\mu Q}(C_c F D_p)\right] \tag{9.17}$$

Cunningham

## Example 9.7 Grade-Efficiency Curve for Single-Stage ESP

The average electric field in a single-stage, plate-wire ESP is 300,000 V/m. The gas flowing through it is air at 298 K and 1 atm. The dielectric constant of the particles is 5.0. The *specific collection area* (SCA = $A_c/Q$) is 78.8 $m^2/(m^3/s)$. Show that the grade efficiency for particulate removal goes through a minimum for particle diameters between 0.1 and 1.0 μm.

## Solution

Equation (9.17) gives

$$\eta(D_p) = 1 - \exp\{-(78.8)(8.85 \times 10^{-12})(3 \times 10^5)^2 C_c F D_p/[3(1.84 \times 10^{-5})]\}$$
$$= 1 - \exp\{-1.137 \times 10^6 C_c F D_p\}.$$

For air at 298 K and 1 atm, $\lambda = 0.0667$ μm. For $\kappa = 5.0$, Eq. (9.16) becomes

$$F = \left(1 + \frac{0.1334}{D_p'}\right)^2 + \frac{8}{7\left(1 + \frac{0.1334}{D_p'}\right)}$$

where $D_p'$ is in microns. The following table summarizes the calculations to estimate the ESP's grade efficiency for various particle sizes.

| $D_p$ (μm) | $C_c$ | $F$ | η |
|---|---|---|---|
| 0.01 | 22.68 | 206.0 | 1.000 |
| 0.05 | 5.06 | 13.77 | 0.981 |
| 0.1 | 2.91 | 5.94 | 0.860 |
| 0.2 | 1.89 | 3.46 | 0.774 |
| 0.4 | 1.42 | 2.64 | 0.819 |
| 0.6 | 1.28 | 2.43 | 0.880 |
| 0.8 | 1.21 | 2.34 | 0.923 |
| 1.0 | 1.17 | 2.30 | 0.953 |
| 2.0 | 1.08 | 2.21 | 0.996 |

Figure 9.4 is a graphical representation of these results. It shows a "window" for particle sizes between 0.1 and 1.0 μm where the penetration increases significantly. This behavior was first documented experimentally by Abbott and Drehmel (1976) and has been observed by many others since.

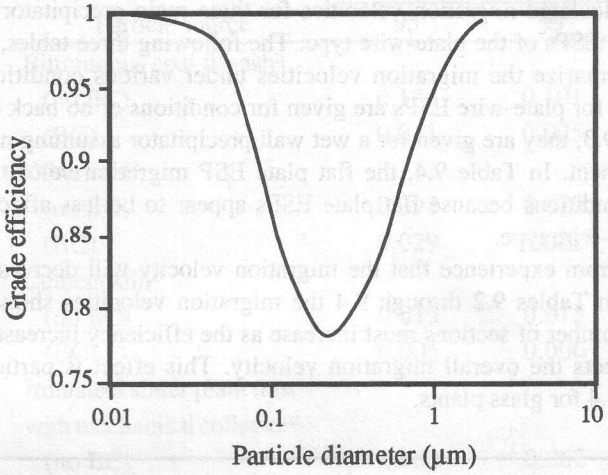


**Figure 9.4** Grade efficiency versus particle size for an ESP

## 9.4 OVERALL EFFICIENCY

**Your objectives in studying this section are to**

1. Estimate the overall efficiency of an ESP with Deutsch-Anderson equation.
2. Estimate the overall efficiency through Gaussian quadrature formulas.

Equation (9.3) as it stands, without refinements, is known as the Deutsch-Anderson equation and has been used as the basis for much work on precipitators. Although it is a grade-efficiency equation, it has been the practice to use it for overall efficiency calculations. This is done by replacing $u_t$ with a so-called *effective migration velocity*, $w_e$. This quantity is taken to represent the collection behavior of an entire dust of a certain kind and under a certain set of operating conditions. It is back calculated from experimental data and so is really a performance parameter. Equation (9.3) becomes:

$$\text{SCA} = \frac{A_c}{Q} = -\frac{\ln(1-\eta_M)}{w_e} \tag{9.18}$$

Turner et al. (1988 a) calculated migration velocities for three main precipitator types: plate-wire, flat plate, and wet wall ESPs of the plate-wire type. The following three tables, keyed to overall design efficiency, summarize the migration velocities under various conditions. In Table 9.2, the migration velocities for plate-wire ESPs are given for conditions of no back corona and severe back corona. In Table 9.3, they are given for a wet wall precipitator assuming no back corona and no rapping reentrainment. In Table 9.4, the flat plate ESP migration velocities are given only for no back corona conditions because flat plate ESPs appear to be less affected by high resistivity dusts than the plate-wire type.

It is generally expected from experience that the migration velocity will decrease with increasing efficiency. However, in Tables 9.2 through 9.4 the migration velocities show some fluctuations. This is because the number of sections must increase as the efficiency increases, and the changing sectionalization affects the overall migration velocity. This effect is particularly noticeable, for example, in Table 9.4 for glass plants.

---

## Example 9.8 Design of Flat Plate ESP Based on Migration Velocity

Calculate the total collector plate area for a flat plate ESP to control fly-ash emissions from a coal-fired boiler burning bituminous coal. The flue gas stream is 24 $m^3/s$ at 436 K. Analysis of the ash shows a resistivity of $1.2 \times 10^{11}$ ohm-cm. The overall efficiency required is 99.9%.

### Solution

Calculate the SCA from Eq. (9.18). The fly-ash migration velocity is 0.160 m/s (see Table 9.4). Then, SCA = –ln (1 – 0.999)/0.16 = 43.2 $m^2/(m^3/s)$. The total collector plate area is then Ac = (43.2)(24) = 1,037 m2.

---

A more general method to calculate overall efficiencies is based on the grade-efficiency equation for the ESP and the size distribution function of the aerosol population entering the device. If the aerosol is log-normally distributed, the calculation of overall efficiency can be done numerically through Gaussian quadrature formulas as shown in Chapter 7.

## Table 9.2 Plate-Wire ESP Migration Velocities (m/s)

| Particle source | Efficiency (%) 95 | 99 | 99.5 | 99.9 |
|---|---|---|---|---|
| Bituminous coal fly-ash[a] | | | | |
| (no BC) | 0.126 | 0.101 | 0.093 | 0.082 |
| (BC) | 0.031 | 0.025 | 0.024 | 0.021 |
| Other coal[a] | | | | |
| (no BC) | 0.097 | 0.079 | 0.079 | 0.072 |
| (BC) | 0.029 | 0.022 | 0.021 | 0.019 |
| Cement kiln[b] | | | | |
| (no BC) | 0.015 | 0.015 | 0.018 | 0.018 |
| (BC) | 0.006 | 0.006 | 0.005 | 0.005 |
| Iron/steel sinter plant dust with mechanical collector[a] | | | | |
| (no BC) | 0.068 | 0.062 | 0.066 | 0.063 |
| (BC) | 0.022 | 0.018 | 0.018 | 0.017 |
| Incinerator fly-ash[c] | | | | |
| (no BC) | 0.153 | 0.114 | 0.106 | 0.094 |

[a] At 420 K. BC = back corona.
[b] At 590 K.
[c] At 395 K.
Source: From Turner, J.H., et al. *JAPCA*, **38**:458 (1988 ). Reprinted with permission from *JAPCA*.

### Example 9.9 Design of ESP Based on Grade-Efficiency Equation

Estimate the overall efficiency of the ESP of Example 9.8 integrating the grade efficiency equation. The particles entering the device are log-normally distributed with MMD = 16 mm and $\sigma_g$ =3.0. The dielectric constant of the particles is 5.0.

### Solution

At a temperature of 436 K, Eq. (9.8) gives the maximum electric field strength, $E_{max} = E_s$ = 433,000 V/m. For a flat-plate configuration with no back corona, Table 9.1 gives $K$ = 1.26. Then, $E_{av}$ = 433,000/1.26 = 344,000 V/m. From Example 9.8, SCA = 43.2 s/m. The sub

## Table 9.3 Wet Wall Plate-Wire ESP Migration Velocities (m/s)

| | Efficiency (%) | | | |
|---|---|---|---|---|
| **Particle source**[a] | 95 | 99 | 99.5 | 99.9 |
| Bituminous coal fly-ash | 0.314 | 0.330 | 0.338 | 0.249 |
| Other coal | 0.400 | 0.427 | 0.441 | 0.314 |
| Cement kiln | 0.064 | 0.056 | 0.050 | 0.057 |
| Iron/steel sinter plant dust with mechanical collector | 0.140 | 0.137 | 0.133 | 0.116 |

[a] All sources at 370 K, no back corona.

Source: From Turner, J. H. et al. *JAPCA*, **38**:458 (1988 ). Reprinted with permission from *JAPCA*.

## Table 9.4 Flat plate ESP migration velocities (m/s).

| | Efficiency (%) | | | |
|---|---|---|---|---|
| **Particle source** | 95 | 99 | 99.5 | 99.9 |
| Bituminous coal fly-ash[a] | 0.132 | 0.151 | 0.186 | 0.160 |
| Other coal[a] | 0.155 | 0.112 | 0.151 | 0.135 |
| Cement kiln[b] | 0.024 | 0.023 | 0.032 | 0.031 |
| Glass plant[c] | 0.018 | 0.019 | 0.026 | 0.026 |
| Iron/steel sinter plant dust with mechanical collector[a] | 0.134 | 0.121 | 0.131 | 0.124 |
| Incinerator fly-ash[d] | 0.252 | 0.169 | 0.211 | 0.183 |

[a] At 420 K, no back corona.

[b] At 590 K, no back corona.

[c] At 530 K, no back corona.

[d] At 395 K, no back corona.

Source: From Turner, J. H. et al. *JAPCA*, **38**:458 (1988 ). Reprinted with permission from *JAPCA*.

program FUNCTION HETA(D) calculates the grade efficiency from Eqs. (9.16) and (9.17). Empirical correlations to estimate the viscosity and the mean-free path for air at atmospheric pressure as a function of temperature are part of the subprogram. The grade efficiency equation is integrated numerically with a 16-point Gauss-Hermite quadrature formula to give an overall efficiency of 99.6%.

```
FUNCTION HETA(D)
   REAL LAMBDA, DIEL, EL, SCA, VIS, E0, T, D
   PARAMETER (E0 = 8.85E-12)
   DATA T, DIEL, EL, SCA /436.0, 5., 3.44E5, 43.2/
   CUN(D)=1.+(2.*LAMBDA/D)*(1.257+.4*EXP(-.55*D/LAMBDA))
   AFAC(D)=(1.+2.*LAMBDA/D)**2+2.*((DIEL-1.)/(DIEL+2.))/
  *     (1.+2.*LAMBDA/D)
   VIS = 1.72E-5*(T/273.0)**0.71
   LAMBDA = 6.71E-11*T**1.21
    IF (0.55*D/LAMBDA .LT. 80. ) THEN
       CUNING=CUN(D)
    ELSE
       CUNING= 1. + 2.*LAMBDA/D
    ENDIF
    ARGUM=SCA*E0*EL**2*CUNING*AFAC(D)*D/(3.*VIS)
    IF (ARGUM .GT. 80.0) THEN
      PEN=0.0
    ELSE
      PEN=EXP(-ARGUM)
    ENDIF
   HETA = 1. - PEN
   END
```

## 9.5 CORRECTIONS TO THE MODEL

**Your objectives in studying this section are to**

1. Identify those phenomena affecting the performance of the ESP not incorporated in the grade-efficiency model.
2. Define the quality factor of the flow distribution and include it in the efficiency calculations.
3. Define the loss factor owing to reentrainment and gas sneakage, and include it in the efficiency calculations.

The experimental values of the effective migration velocity do not behave in all respects as predicted by the theoretical model. There are various aspects of the performance of an ESP not incorporated in the model. These are sometimes referred to as non-Deutschian phenomena. Some of the most significant are *non-uniform gas velocity distribution; gas sneakage;* and *rapping reentrainment*. Possible corrections to the model for these items follow.

### 9.5.1 Non-Uniform Gas Velocity Distribution

The theoretical model developed assumes that the fluid velocity parallel to the collector surface is everywhere the same and equal to the volumetric flow rate divided by the total cross-sectional area. This condition is almost impossible to achieve in practice. Uniform, low-turbulence gas flow is very important for optimum precipitator performance. The detrimental effect of non-uniform gas flow is twofold. First, owing to the exponential nature of the collection mechanism uneven treatment of the gas lowers collection efficiency in the high-velocity zones to an extent not compensated for in the low-velocity zones. Second, high-velocity regions near collection plates can sweep particles back into the main gas stream.

Although it is known that a poor gas velocity distribution results in reduced collection efficiency, it is difficult to formulate a mathematical description for gas flow quality. The following development, presented by McDonald and Dean (1982), demonstrates the general considerations to be made in accounting for the effects of a non uniform gas velocity distribution on collection efficiency. Eq. (9.18) can be written as

$$Pt^{id} = \exp\left(-\frac{A_c w_e}{A_1 v_a}\right) = \exp\left(-\frac{k}{v_a}\right) \tag{9.19}$$

where

$Pt^{id}$ = ideal overall penetration
$A_1$ = inlet cross sectional area
$v_a$ = average gas inlet velocity
$k = A_c w_e / A_1$

The precipitator can be divided into a number of imaginary channels corresponding to pitot tube traverse points. The penetration for all the channels can be summed and averaged to obtain the mean penetration with an actual velocity distribution instead of an assumed uniform velocity.

$$Pt = \frac{1}{N v_a} \sum_{j=1}^{N} v_j Pt_j^{id} = \frac{1}{N v_a} \sum_{j=1}^{N} v_j e^{-\frac{k}{v_j}} \tag{9.20}$$

where

$N$ = number of points for velocity traverse
$v_j$ = point values of gas velocity

For any practical velocity distribution and efficiency, the mean penetration calculated in this manner will be higher than that calculated based on an average uniform velocity. This is equivalent to a reduced "apparent" migration velocity. The ratio of the original migration velocity to the "apparent" migration velocity is called the *quality factor* $\phi$, of the velocity distribution. Equation (9.20) can, then, be written as:

$$Pt = \exp\left(-\frac{k}{\phi v_a}\right) = \frac{1}{N v_a} \sum_{j=1}^{N} v_j e^{-\frac{k}{v_j}} \tag{9.21}$$

Solving Eq. (9.21) for the quality factor,

$$\phi = -\frac{k}{v_a \ln\left[\frac{1}{N v_a} \sum_{j=1}^{N} v_j e^{-\frac{k}{v_j}}\right]} = \frac{\ln\left(Pt^{id}\right)}{\ln\left(Pt\right)} \tag{9.22}$$

The use of Eq. (9.22) with measured velocity traverses in a working precipitator may yield values of $\phi$ as high as 2 to 3 in a poorly regulated flow pattern (McDonald and Dean 1982). When care is taken, through scale model studies, values of $\phi$ as low as 1.1 or 1.2 should be achieved (Licht 1980).

---

## Example 9.10 Flow Quality Factor Calculations

(a) The ideal overall penetration for an ESP is 1% assuming a uniform velocity distribution. There are actually three zones of equal flow area in which $v_1 = v_a/2$, $v_2 = v_a$, and $v_3 = 3v_a/2$. Calculate the flow quality factor and the actual overall penetration.
(b) The ideal overall penetration for an ESP is 1% assuming a uniform velocity distribution. The flow quality factor is 2.0. Calculate the actual overall penetration.

### Solution

(a) From Eq. (9.19), $k/v_a = -(\ln Pt^{id}) = -\ln(0.01) = 4.605$. The following table summarizes the calculations for the quality factor and actual penetration:

| $j$ | $v_j/v_a$ | exp $(-k/v_j)$ | $v_j/v_a \exp(-k/v_j)$ |
|---|---|---|---|
| 1 | 0.5 | 0.0001 | 0.00005 |
| 2 | 1.0 | 0.01 | 0.01 |
| 3 | 1.5 | 0.0447 | 0.06705 |
| | | | $\Sigma = 0.07710$ |

From Eq.(9.21), $Pt = \Sigma/N = 0.0771/3 = 0.0257$. Equation (9.22) yields $\phi = \ln(0.01)/\ln(0.0257) = 1.258$.

(b) From Eq. (9.22), $Pt = (Pt^{id})^{1/\phi} = (0.01)^{0.5} = 0.10$.

## Comments

These examples emphasize the importance of a uniform velocity distribution in an ESP's performance. Part b shows a 10-fold increase in penetration for a flow quality factor of 2.0! However, Hein (1989) developed a computer model that shows the possibility of improving the performance of an ESP by using a controlled non-uniform gas distribution at the inlet and outlet faces of the precipitator when there are significant rapping reentrainment losses.

### 9.5.2 Sneakage and Rapping Reentrainment

Sneakage and rapping reentrainment losses are best considered on the basis of the sections within an ESP. Consider first the effect of sneakage. Assuming that the gas is well mixed between sections, the penetration for each section can be expressed as:

$$Pt_s = S_N + (1 - S_N)Pt_c(Q') \tag{9.23}$$

where

$Pt_s$ = section's overall penetration
$S_N$ = fraction of the gas bypassing the section (sneakage)
$Q'$ = gas volume flow in the collection zone = $Q(1 - S_N)$
$Pt_c\,(Q')$ = overall penetration in the collection zone

The penetration for the entire ESP is the product of the section penetrations. The sneakage sets a lower limit on the collection efficiency through each section.

The collected dust accumulates on the plates until they are rapped, when most of the material falls into the dust hopper. A fraction of it is reentrained by the gas flow and leaves the section. The average penetration for a section, including sneakage and reentrainment is

$$Pt_s = S_N + (1 - S_N)Pt_c(Q') + RR\{(1 - S_N)[1 - Pt_c(Q')]\} \tag{9.24}$$

where $RR$ = fraction reentrained. Equation (9.24) can be written as

$$Pt_s = LF + (1 - LF)Pt_c(Q') \tag{9.25}$$

where $LF$ (loss factor) is defined as

$$LF = S_N + RR - (S_N)(RR) \tag{9.26}$$

Fly-ash precipitators analyzed in this way have average values of $S_N = 0.07$, $RR = 0.12$, and $LF = 0.182$ (Turner et al. 1988 a). To achieve a given overall penetration, choose the minimum number of sections, $N_s$, such that:

$$N_s > \frac{\ln(Pt)}{\ln(LF)} \tag{9.27}$$

## Example 9.11 Sneakage and Reentrainment Losses

Estimate the minimum number of sections for a fly-ash ESP if the overall efficiency must be 99.9%. Assume that the loss factor owing to sneakage and reentrainment is 0.182. Assuming that all the sections have the same overall penetration, estimate the penetration in the collection zone, $Pt_c$, of each section.

### Solution

Equation (9.27) gives $N_s > \ln(1 - 0.999)/\ln(0.182) = 4.06$. Therefore, the ESP should have 5 sections. Assuming that all the sections have the same overall penetration,

$$Pt_c = \frac{Pt^{(1/N_s)} - LF}{1 - LF} \tag{9.28}$$

Substituting in Eq. (9.28), $Pt_c = [(0.001)0.2 - 0.182]/(1 - 0.182) = 0.0846$.

## Example 9.12 Corrections to Penetration Predicted by the ESP Model

The collection area of the ESP of Example 9.9 is equally divided into six sections in the direction of the gas flow. Values for sneakage and rapping reentrainment are 10% and 12%, respectively; the flow quality factor is 1.2. Estimate the actual overall collection efficiency for the ESP.

### Solution

The penetration predicted by Feldman's model, $Pti^d$, must be corrected for non-uniform gas flow distribution, number of sections, and reduced gas flow—owing to sneakage—through the collection zone. The corrected value corresponds to $Pt_c$, and is given by

$$Pt_c = \left(Pt^{id}\right)^{1/[\phi N_s(1 - S_N)]} \tag{9.29}$$

Substituting in Eq. (9.29), $Pt_c = (0.004)^{1/[(1.2)(6)(0.9)]} = 0.426$. The loss factor is $LF = 0.10 + 0.12 - (0.1)(0.12) = 0.208$. From Eq. (9.25), $Pt_s = 0.545$, then $Pt = (0.545)^6 = 0.026$, and $\eta_M = 97.4\%$.

## Example 9.13 Design of ESP Including Corrections to Model

Consider the conditions of Examples 9.9 and 9.12. Redesign the ESP to maintain an actual overall collection efficiency of 99.6%.

### Solution

Equation (9.27) gives the optimum number of sections the ESP should have: $N_s > \ln(0.004)/\ln(0.208) = 3.52$. Therefore, $N_s = 4$ sections. Equation (9.28) gives the actual overall penetration in the collection zone of each of the ESP's sections: $Pt_c = [(0.004)^{0.25} - 0.208]/(1 - 0.208) = 0.055$. Eq. (9.29), applied to a single section, gives $Pt^{id} = Pt_c^{\phi(1 - SN)} = (0.055)^{1.056} = 0.0468$. The computer program ESP calculates the collection area per section

for a given value of $Pt^{id}$, as predicted by Feldman's model. The answer is 324.3 $m^2$/section. For four sections, the total collection area is 1,297.2 $m^2$.

```
      PROGRAM ESP
C
C     CALCULATES THE COLLECTION AREA REQUIRED FOR A GIVEN IDEAL
C     PENETRATION, PENID, AS PREDICTED BY FELDMAN'S MODEL
C
      REAL PENID, MMD, NMD, SIGG, Q, LAMBDA, VIS, X1, X2, SL
      REAL RTBIS, XACC, EL, CUN, AFAC, PEN, DIEL
      INTEGER N
      LOGICAL SUCCES
      COMMON /BLOCK1/ PENID, MMD, SIGG, Q, LAMBDA, VIS, EL, DIEL, E0
      EXTERNAL FUNCP
      CUN(D)=1.+(2.*LAMBDA/D)*(1.257+.4*EXP(-.55*D/LAMBDA))
      AFAC(D)=(1.+2.*LAMBDA/D)**2+2.*((DIEL-1.)/(DIEL+2.))/
     *      (1.+2.*LAMBDA/D)
      X1=-3.*VIS*Q*LOG(PENID)/(E0*EL**2*CUN(MMD)*AFAC(MMD)*MMD)
      X2=SIGG*X1
      CALL ZBRAC(FUNCP, X1, X2, SUCCES)
      IF (SUCCES) THEN
        XACC=ABS((X1-X2)/10000.)
        SL=RTBIS(FUNCP, X1, X2, XACC)
        PRINT *, ' COLLECTION AREA PER SECTION  ', SL, ' SQ METERS'
        GO TO 10
      ENDIF
      PRINT *, 'FAILURE IN BRACKETING SL '
10    STOP
      END
C
      BLOCK DATA
      REAL PENID, MMD, SIGG, Q, LAMBDA, VIS, EL, DIEL, E0
      COMMON /BLOCK1/ PENID, MMD, SIGG, Q, LAMBDA, VIS, EL, DIEL, E0
      DATA PENID/0.0468/, MMD/16.0/, SIGG/3.0/, Q/24.00/, LAMBDA/
     *    0.1050/, VIS/2.4E-5/, EL/3.44E5/, DIEL/5./, E0/8.85E-18/
      END
C
      FUNCTION FUNCP(SL)
      REAL PENID, MMD, SIGG, Q, LAMBDA, VIS, EL, DIEL, E0, PEN, X, A
      REAL NMD, EPS, PENC, FUNCP, SL
      INTEGER N
      COMMON /BLOCK1/ PENID, MMD, SIGG, Q, LAMBDA, VIS, EL, DIEL, E0
      PARAMETER (N=10, EPS=1.0E-06)
      DIMENSION X(N), A(N)
```

```
      CUN(D)=1.+(2.*LAMBDA/D)*(1.257+.4*EXP(-.55*D/LAMBDA))
      AFAC(D)=(1.+2.*LAMBDA/D)**2+2.*((DIEL-1.)/(DIEL+2.))/
     *     (1.+2.*LAMBDA/D)
      CALL HERMIT(N, X, A, EPS)
      NMD=EXP(LOG(MMD)-3*(LOG(SIGG))**2)
      SUMA=0.0
      DO 10 I=1, N
        D=EXP(SQRT(2.)*LOG(SIGG)*X(I)+LOG(NMD))
        IF (0.55*D/LAMBDA .LT. 80. ) THEN
          CUNING=CUN(D)
        ELSE
          CUNING= 1. + 2.*LAMBDA/D
        ENDIF
        ARGUM=SL*E0*EL**2*CUNING*AFAC(D)*D/(3.*Q*VIS)
        IF (ARGUM .GT. 80.0) THEN
          PEN=0.0
        ELSE
          PEN=EXP(-ARGUM)
        ENDIF
        SUMA=SUMA+A(I)*PEN*EXP(3.*SQRT(2.)*LOG(SIGG)*X(I))
   10   CONTINUE
      PENC=SUMA/(SQRT(3.1416)*EXP(4.5*(LOG(SIGG))**2))
      FUNCP=PENC-PENID
      END
```

## 9.6 PRACTICAL DESIGN CONSIDERATIONS

**Your objectives in studying this section are to**

1. Estimate the dimensions of an ESP, given the collection area.
2. Estimate the total power consumption of an ESP.
3. Understand the importance of flue gas conditioning to maintain proper resistivity of the collected dust.

The complete design of an ESP includes sizing and determining the configuration of the collecting and discharge electrodes, calculating the power consumption, and specifying rapping, dust removal, and flue gas conditioning systems.

### 9.6.1 Sizing the electrodes

The discharge electrode system is designed in conjunction with the collection electrode system to maximize the electric current and field strength. The shape of the discharge electrode may be in the form of cylindrical or square wires, barbed wire, or stamped from formed strips of metal of various shapes. Most ESPs in the U.S. use cylindrical wires of about 2.5 mm diameter kept taut by weights, whereas European designs favor rigid, mast-type supports for the wires. Recent designs in both continents use rigid discharge electrodes (Cooper and Alley 1986).

The number and size of the collection plates depend on the total collection area specified, the gas flow velocity, the plate spacing, and the aspect ratio (length-height). An ESP collecting a dry particulate material runs a risk of nonrapping, continuous reentrainment if the gas velocity becomes too large. For fly-ash applications, the maximum acceptable velocity is about 1.5 m/s for plate-wire ESPs and about 1 m/s for flat-plate ESPs.

Most U.S. utility precipitators have 230-mm plate spacing, although systems purchased in the last few years generally have 300-mm spacing which allows the use of rigid discharge electrodes. A few U.S. utilities are currently installing ESPs with the new European plate spacing standard of 400 mm (Offen and Altman 1991).

The Deutsch equation relates ESP performance to specific collecting surface area with no regard to the length-height aspect ratio. However, because of gas sneakage and rapping reentrainment losses, the actual precipitator's performance is dependent on how the surface is arranged. For collection efficiencies grater than 99%, the aspect ratio should be kept above 1.0.

The number of ducts for gas flow, Nd, is given by

$$N_d = \frac{Q}{2 W v_a H} \tag{9.30}$$

where

$W$ = wire-plate spacing

$H$ = plate height

Since each plate has two collecting surfaces, the total collection area is given by

$$A_c = 2 N_d R H^2 \tag{9.31}$$

where $R$ is the aspect ratio. Combining Eqs. (9.30) and (9.31), the plate height is

$$H = \frac{(\mathrm{SCA}) v_a W}{R} \tag{9.32}$$

### Example 9.14 Dimensions of Plate-Wire ESP

Estimate the dimensions of a plate-wire ESP treating 333 $m^3/s$ of gas with a total plate area of 14,000 $m^2$ for 99% collection of fly-ash. Plate spacing must be 300 mm to allow the use of rigid discharge electrodes.

### Solution

Choose typical values of gas velocity and aspect ratio: $v_a = 1.5$ m/s, $R = 1.0$. Calculate SCA $= A_c/Q = 14{,}000/333 = 42.0$ s/m. For a wire-plate spacing of 150 mm, Eq. (9.32) gives $H =$ 9.45 m. Since the aspect ratio is unity, $L = H = 9.45$ m. Equation (9.30) gives $N_d = 78.3$; choose $N_d = 79$ ducts. The width of the ESP is (79)(0.30) = 23.7 m.

Because the number of ducts was rounded to the next integer, the actual collection area is higher than that specified based on collection efficiency (14,110 $m^2$ versus 14,000 $m^2$), and the gas velocity is lower than the value initially chosen (1.49 m/s versus 1.5 m/s). Both factors improve the performance of the ESP. Figure 9.5 is a schematic diagram of the resulting design.

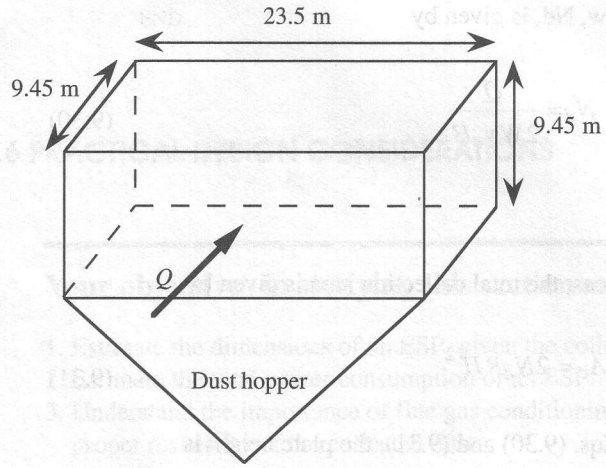


**Figure 9.5** Dimensions of the ESP of Example 9.14

## 9.6.2 Power consumption

The two main sources of power consumption of an ESP are from corona power and gas pressure drop. Total pressure drop for a precipitator and associated ductwork is usually of the order of 1.0 kPa (Turner et al. 1988 a). Corona power is a strong function of overall penetration.

The following correlation is based on actual operational data presented by White (1984):

$$\dot{W}_c = Q\left(115.8 + \frac{1.17}{Pt}\right) \tag{9.33}$$

where $\dot{W}_c$ is the corona power in watts.

---

### Example 9.15 Power Consumption of ESP

Estimate the total power consumption of the ESP of Example 9.14. Assume that the motor-fan efficiency is 60%.

### Solution

Assume a pressure drop of 1.0 kPa. The fan power is (333)(1.0)/(0.6) = 555 kW. Equation (9.33) gives the corona power, $\dot{W}_c$ = 333(115.8 + 1.17/0.01) = 77.5 kW. The total power is 632.5 kW.

---

## 9.6.3 Flue Gas Conditioning Systems

The major factors affecting fly-ash resistivity are temperature and chemical composition (of the fly-ash and of the combustion gases). For a given chemical composition, fly-ash resistivity always exhibits a distinct maximum at temperatures about 395 to 450 K. The temperature of the maximum resistivity is unfortunate for power boiler operators. ESP operating temperatures cannot be much below 395 K without risking condensation of sulfuric acid on some of the colder surfaces. Conversely, operating at temperatures much higher than 450 K results in unnecessary loss of heat out the stack, reducing the thermal efficiency of the plant (Cooper and Alley 1986).

Resistivity decreases with increased fuel sulfur content. because of increased adsorption of conductive gases, such as $SO_3$, by the fly-ash. The combustion of high-sulfur coal (>2% sulfur) produces sufficient $SO_3$ to condition the fly-ash to a low resistivity, as shown on Figure 9.6. The combustion of low-sulfur coals (<1% sulfur) with highly alkaline ash produces only small amounts of $SO_3$, resulting in very high ash resistivities. In the intermediate case, the existing data for medium-sulfur coal exhibit considerable scatter in the relationship between the $SO_2$ and $SO_3$ in the gas entering the ESP (Harrison et al. 1988). The Clean Air Act Amendments of 1990 require electric utilities to reduce $SO_2$ emissions by approximately 10 million ton/yr by 2000. Many existing plants are switching to low-sulfur coal, with negative impacts on the electrical operation of ESPs.

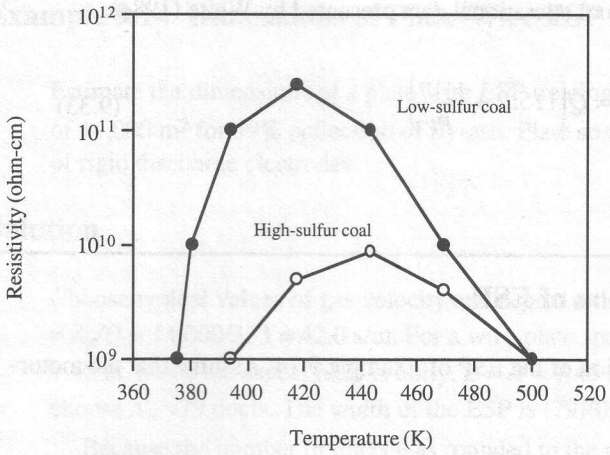


**Figure 9.6** The effect of temperature and fuel sulfur content on fly ash resistivity

Other $SO_2$ "dry" reduction strategies, such as spray dryers, furnace sorbent injection, and conversion to fluidized-bed combustion, have a significant impact of ESPs located downstream. These techniques increase the particulate loading and change the resistivity of the collected material, generally making it more difficult to remove. Durham et al. (1990) reported resistivity values of sorbent–fly-ash mixtures of the order of $10^7$ to $10^9$ ohm-cm at spray dryer conditions. Although the injected material had a high resistivity at 420 K, the surface conditioning provided by the increased moisture and cooling was sufficient to reduce it dramatically. At such low resistivities, the electrostatic force holding the particles onto the collector plates is reduced and the particles are easily reentrained. They found that reentrainment had to account for 60% of the observed penetration per section to correctly predict ESP performance at spray dryer conditions (see Problem 9.19).

The cohesive characteristics of the sorbent–fly-ash mixture improve by using additives such as ammonia. The interaction of ammonia and $SO_3$ results in the formation of ammonium bisulfate and sulfate, which condense on the surface of the particles. These surface deposits are viscous and cohesive, which reduce rapping and nonrapping reentrainment.

The *atmospheric fluidized-bed combustor* (AFBC) is an emerging technology for the control of $SO_x$ and $NO_x$ emissions from coal-fired power plants. Crushed coal is fed into a bed of inert ash mixed with limestone or dolomite. The bed is fluidized by injecting air through the bottom at a controlled rate. The coal burns within the bed and the $SO_x$ formed reacts with the limestone to form a dry calcium sulfate which is removed with the fly-ash in a downstream particulate collection device. The system can remove up to 95% of the $SO_2$ and up to 80% of the $NO_x$ emissions (U.S. Congress, 1991). However, Altman (1988) reported severe ESP operational problems at a full-scale coal-fired power plant converted to AFBC operation due to the high resistivity of the collected dust. Flue gas conditioning to reduce the particulate resistivity was been considered.

Gas conditioning equipment is frequently used to upgrade existing ESPs. Conditioning agents used include $SO_3$, $H_2SO_4$, sodium compounds, and ammonia. A typical dose rate of the gaseous agents is 10 to 30 ppm by volume. There are several vendors and systems commercially available. Gas conditioning usually gives good results with reasonably small expense.

## 9.7 COSTING CONSIDERATIONS

**Your objectives in studying this section are to**

1. Estimate the TCI for various types of ESPs.
2. Estimate the TAC for electrostatic precipitation.

This section presents methods to estimate the total capital investment and total annual costs for an ESP system. This material is taken primarily from Turner et al. (1988b).

### 9.7.1 TCI

The TCI includes costs for the ESP structure, the internals, rappers, power supply, auxiliary equipment, and the usual direct and indirect installation costs. Land, working capital, and offsite facilities are not normally required.

ESP equipment costs are almost always correlated with the collecting area. Turner et al. (1988 b) obtained cost quotes from precipitator vendors and regressed them against their collecting areas. These costs, updated to June 1990, are given by

$$EC = aA_c^b \tag{9.34}$$

where

$A_c$ = collecting area, $m^2$

$a$, $b$ = regression parameters

Table 9.5 lists the values of $a$ and $b$ for different ranges of collecting area.

**Table 9.5 Regression Parameters for ESP Equipment Cost Equation[a]**

| Plate area ($m^2$) | $a$ | $b$ |
|---|---|---|
| 930 to 4,600 | 4,551 | 0.6276 |
| 4,600 to 93,000 | 715 | 0.8431 |

Source: From Turner, J. H. et al. *JAPCA*, **38**:715(1988 ). Reprinted with permission from *JAPCA*. [a]Updated to June 1990.

These costs apply to all ESP configurations, except the two-stage. They include the following: ESP casing, pyramidal hoppers, rigid electrodes and internal collecting plates, transformer-rectifier (TR) sets and microprocessor controls, rappers, inlet and outlet nozzles and diffuser plates, weather enclosure and stair access, structural supports, and insulation (7.6 cm of fiberglass encased in a metal skin).

Two-stage ESPs are usually limited to small sizes and are sold as modular units. To be consistent with industry practice, the equipment costs (in $ of June 1990) are given as a function of flow rate through the unit (Turner et al. 1988b),

$$EC = 27{,}200 + 41{,}500 \ln Q \qquad 1.0 < Q, \frac{m^3}{s} < 6.0 \qquad (9.35)$$

where $Q$ is the actual volume flow rate through the unit. This cost is for modular units fully assembled mechanically and electrically, and mounted on a steel structural skid.

The purchased equipment cost, $B$, is the sum of the equipment cost, auxiliary equipment, instruments and controls, taxes, and freight. TCI is estimated from a series of factors applied to the purchased equipment cost to obtain direct and indirect costs for installation. Table 9.6 summarizes the most important factors for average installation conditions. For two-stage ESPs, purchased as packaged systems, installation costs are greatly reduced. Turner et al. (1988b) suggest that, in this case, TCI = 1.25$B$.

### 9.7.2 TAC

Direct annual costs include operating and supervisory labor, maintenance (labor and materials), utilities, dust disposal, and waste water treatment for wet ESPs. Typical operating labor requirements are 2 h/shift. Supervisory labor is taken as 15% of operating labor. Maintenance labor is estimated as 660 h/yr; annual maintenance materials are approximately 1% of the purchased equipment cost.

If the collected dust cannot be recycled or sold, it must be disposed of. Disposal costs for nonhazardous wastes are typically $30/metric ton. Disposal of hazardous wastes may cost 10 times as much. If the dust collected can be reused or sold, a recovery credit should be taken.

For capital recovery calculations, ESP systems are assumed to have average lifetimes of 20 yr. Overhead is calculated as 60% of total labor plus maintenance materials. Property taxes, insurance, and administrative charges are estimated as 4% of the TCI.

---

### Example 9.16 Capital Investment and Annual Cost of ESP

Assume a plate-wire ESP is required for the control of fly-ash emissions from a coal-fired boiler burning bituminous coal. The flue gas stream is 26.3 m³/s at 435 K and has an inlet

**Table 9.6 Capital Cost Factors for ESPs**

| Costs | Factor |
|---|---|
| Direct costs | |
| ESP and auxiliary equipment costs | $A$ |
| Instruments and controls | $0.10A$ |
| Taxes | $0.03A$ |
| Freight | $0.05A$ |
| Purchased equipment cost | $B = 1.18A$ |
| Installation direct costs | $0.67B$ |
| Total direct costs | $1.67B + SP^a + Bldg^b$ |
| Indirect costs | $0.57B$ |
| TCI | $2.24B + SP + Bldg$ |

Source: Vatavuk and Neveril (1980). [a]Site Preparation. [b]Buildings.

ash loading of 0.01 kg/m$^3$. The design SCA for 99.9% overall efficiency is 62.4 s/m. Estimate the TCI and TAC for this application. Assume that the unit operates for 8,640 h/yr. Operating labor rate is \$15/h, maintenance labor rate is \$20/h. The cost of electricity is \$0.06/kW-h, dust final disposal costs are \$30/metric ton. The minimum attractive rate of the return is 12%/yr. Assume that no buildings or special site preparation is needed. Auxiliary equipment needed—ductwork, fan, motor, and stack—cost \$65,000.

## Solution

The total collection area is (62.4)(23.6) = 1,473 m$^2$. From Eq. (9.34) and Table 9.5, $EC$ = 4,551 $(1473)^{0.6276}$ = \$443,100. The sum of the ESP and auxiliary equipment costs is $A$ = 443,100 + 65,000 = \$508,100. From Table 9.6, the purchased equipment cost is $B$ = 1.18 (508,100) = \$600,000. TCI = 2.24 (\$600,000) = \$1,344,000 (\$ of June 1990).

Assuming a total pressure drop of 1.0 kPa and a mechanical efficiency of 60 percent for the fan, the total fan and corona power requirements are given by [(1.0)(23.6)/0.6] + 23.6 [0.1158 + (0.00117/0.001)] = 70 kW. The total mass of dust collected yearly is (26.3)(0.01) (0.999)(3,600)(8,640)/1,000 = 7,330 metric ton. For a useful life of 20 yr and a yearly rate of return of 12%, the capital recovery factor is 0.1339/yr. The following table presents annual costs for this project.

| Item | Annual cost ($/yr) |
|---|---|
| Direct annual costs | |
| Operating labor: (3)(360)(15) = | 16,200 |
| Supervisory: (0.15)(16,200) = | 2,400 |
| Maintenance labor: (660)(20) = | 13,200 |
| Maintenance materials: (0.01)(600,000) = | 6,000 |
| Electricity: (70)(8,640)(0.06) = | 40,000 |
| Waste disposal: (7,330)(30) = | 219,900 |
| Total direct annual costs | 297,700 |
| Indirect annual costs | |
| Overhead : (0.6)(37,800) = | 22,680 |
| Tax, insurance, administration: (0.04)(1,344,000) = | 53,760 |
| Capital recovery cost: (0.1339)(1,334,000) = | 178,600 |
| Total indirect annual costs | 255,040 |
| TAC | $552,740 |

## 9.8 CONCLUSION

The selection of particulate control equipment in the near future will depend largely on regulatory trends and the technical and commercial success of ongoing particulate control research and development efforts. Well-designed modern ESPs can meet emission targets lower than the current NSPS. Requirements for greater particulate reductions or stringent emission limits based on respirable particulates may limit the use of conventional ESPs. Several options for significantly enhancing precipitators collection efficiency presently under active consideration are wet ESPs; pulse energization tuned specifically for fine particle control; and the addition of a very compact pulse jet baghouse (to be described in detail in Chapter 10) as a polishing step following an ESP.

ESPs have been the workhorse of particulate control equipment for almost a century. However, their future is uncertain and will depend on the ability of researchers and manufacturers to retain the reliability and simplicity of current designs while improving their tolerance to variations in particulate characteristics.

## REFERENCES


Abbott, J. H., and Drehmel, D. C. *Chem. Eng. Prog.*,**72**:47 (1976).

Altman R. F. *JAPCA*, **38**:1455 (1988).

Cochet, R. *Colloq. Intern. Centre Natl.Rech. Sci.*[Paris], **102:**331 (1961).

Cooper, C. D., and Alley, F. C. *Air Pollution Control: A Design Approach,* PWS Engineering, Boston, MA (1986).

Crawford, M. *Air Pollution Control Theory*, McGraw-Hill, New York (1976).

Durham, M. D., Rugg, D. E., Rhudy, R. G., and Puschaver, E. J. *J. Air Waste Manage. Assoc.*, **40**:112 (1990).

Feldman, P. L. Paper No. 75-02.3, 68th Annual Meeting, *Air Pollution Control Association*, Boston, MA (1975).

Flagan, R. C., and Seinfeld, J. H. *Fundamentals of Air Pollution Engineering*, Prentice Hall, Englewood Cliffs, NJ (1988).

Harrison, W. A., Nicholson, J. K., DuBard, J. L., Carlton, J. D., and Sparks, L. E. *JAPCA,* **38**:209 (1988).

Hein, A. G. *JAPCA*, **39**:766 (1989).

Licht, W. *Air Pollution Control Engineering: Basic Calculations for Particulate Collection*, Marcel Dekker, New York (1980).

McDonald, J. R., and Dean, A. H. *Electrostatic Precipitator Manual,* Noyes Data Corporation, Park Ridge, NJ (1982).

Offen, G. R., and Altman R. F. J. *Air Waste Manage.Assoc.*,.**41**:222 (1991).

Turner, J. H., Lawless, P. A., Yamamoto, T., Coy, D. W., Greiner, G. P., McKenna, J. D., and Vatavuk, W. M. *JAPCA*, **38:**458 (1988a).

Turner, J. H., Lawless, P. A., Yamamoto, T., Coy, D. W., Greiner, G. P., McKenna, J. D., and Vatavuk, W. M. *JAPCA,* **38**:715 (1988b).

U.S. Congress, Office of Technology Assessment, *Energy Technology Choices*: *Shaping Our Future,* OTA-E-493, Washington, DC (1991).

Vatavuk, W. M., and Neveril, R. B. *Chemical Engineering,* pp. 157-162 (November 3, 1980).

White, H. J. "Control of Particulates by Electrostatic Precipitation," Chap.12 in *Handbook of Air Pollution Technology*, S. Calvert and H. M. Englund (Eds.), Wiley, NewYork (1984).

White, H. J. *Industrial Electrostatic Precipitation* Addison-Wesley, Reading, MA (1963).

## PROBLEMS

**The problems at the end of each chapter have been grouped into four classes (designated by a superscript after the problem number)**

Class a: Illustrates direct numerical application of the formulas in the text.
Class b: Requires elementary analysis of physical situations, based on the subject material in the chapter.
Class c: Requires somewhat more mature analysis.
Class d: Requires computer solution.

**9.1[a]. Terminal velocity of a charged particle in an electric field**

Repeat Example 9.1 for 2.0-μm diameter particles. Assume that the particle charge is proportional to its surface area. Estimate the terminal velocity of the particles.

*Answer: 0.375 m/s*

**9.2[a]. Dimensions of a tubular ESP**

A small tubular ESP is to produce a collection efficiency of 99% when handling 0.25 $m^3/s$ of air at 773 K and 1 atm containing 2.5-μm particles. The strength of the electric field is 200,000 V/m and the particle charge is $10^{-15}$ C. Determine the dimensions of the ESP. The velocity of the gases through the precipitator must not exceed 0.318 m/s.

*Answer:* L = *1.28 m*

**9.3[b]. ESP overall efficiency to satisfy NSPS**

Consider the coal-fired power plant of Example 5.1. Assuming that 25% of the ash drops out of the furnace as slag, calculate the efficiency of an ESP to remove fly-ash if the plant is to meet the 1980 federal NSPS for particulates.

*Answer: 99.61%*

**9.4[a]. Corona onset value in plate-wire ESP**

A plate-wire ESP handles air at 700 K and 101.3 kPa. The plate spacing is 460 mm and the diameter of the discharge wires is 5 mm. Estimate the corona onset voltage.

*Answer: 17,300 V*

**9.5[a]. Average electric field in a plate-wire ESP**

Estimate the average electric field and the operating voltage for the ESP of Problem 9.4. The resistivity of the collected dust is $10^{12}$ ohm-cm.

*Answer: 119 kV/m*

**9.6[a]. Average electric field in a flat plate ESP**

Repeat Problem 9.5 but for a flat-plate ESP configuration.

*Answer: 165 kV/m*

**9.7[a]. Particle saturation charge**

Determine the time constant and saturation charge for field charging of 5.0-μm par-

ticles having a dielectric constant of 4.0 if the ion concentration is $10^{16}$ ions/m$^3$ and the field strength is 150 kV/m. Assume that the ion mobility is $2.2 \times 10^{-4}$ m$^2$/V-s.

*Answer: 0.21 fC*

**9.8[a]. Total particle charge according to Feldman**

Estimate the total charge on the particles of Problem 9.7 according to Eq. (9.14) for a charging time of 0.1 s. Assume that the gas mean-free path is 0.1 μm.

*Answer: 0.215 fC*

**9.9[b]. Effect of gas flow rate on ESP grade efficiency**

Consider the ESP of Example 9.7. If the gas flow rate increases by 20 percent, estimate the percent increase in penetration for 1.0-μm particles.

*Answer: 66.5%*

**9.10[b]. Effect of average electric field strength on ESP performance**

Consider the ESP of Example 9.7. If the average electric field strength decreases by 20%, estimate the percent increase in penetration for 1.0-μm particles.

*Answer: 200%*

**9.11[a]. Effective migration velocity**

Estimate the effective migration velocity for the fly-ash of Example 9.9.

*Answer: 0.128 m/s*

**9.12[a]. ESP for the control of emissions from a cement kiln**

The gases from a cement kiln flow at a volumetric rate of 380 m$^3$/min at 590 K and 1 atm. A plate-wire ESP will remove 99.9% of the particulate matter carried by the gases. Assuming no back corona, estimate the total collection area based on the effective migration velocities of Table 9.2.

*Answer: 2,430 m$^2$*

**9.13[b]. Effect of sulfur content of the fuel on ESP performance**

Selzler and Watson (*JAPCA*, **24**:115, 1974) proposed the following empirical Deutsch-type equation for the overall penetration of an ESP for the control of fly-ash emissions from a pulverized coal-fired furnace:

$$Pt_M = \exp\left[-0.0456(\text{SCA})^{1.4}\left(\frac{KW}{Q}\right)^{0.6}\left(\frac{S}{AH}\right)^{0.22}\right]$$

where

SCA = specific collection area, s/m

$Q$ = gas volumetric flow rate, $m^3/s$

$KW$ = power input to the discharge electrode, kW

$S$ = sulfur content of the fuel, weight percent

$AH$ = ash content of the fuel, weight percent

(a) A precipitator with an overall efficiency of 97.7% operates on a coal with a sulfur-to-ash ratio of 1.5 : 12.3. To help meet $SO_2$ emissions standards, a coal is substituted with a sulfur-to-ash ratio of 0.8 : 12.5. If all the other operating variables are the same, estimate the new collection efficiency.

*Answer: 96.2%*

(b) What percent change in corona power is necessary if, for the new sulfur-to-ash ratio, it is desired to restore the collection efficiency to its original value?

*Answer: 26.7% increase*

**9.14[a]. Corona power for a fly-ash ESP**

Problem 9.13 gives Selzler and Watson's empirical equation for the overall collection efficiency of an ESP. A precipitator treats 1,322 $m^3/s$ of flue gas to remove fly-ash particles from a pulverized coal-fired power plant. The design overall removal efficiency is 99.5%. The total collection area is 79,320 $m^2$; the coal contains 1.0% S and 12% ash. Estimate the corona power for these conditions.

*Answer: 650 kW*

### 9.15[d]. Effect of back corona on plate-wire ESP performance

Consider the conditions described in Example 9.9. Assuming that a plate-wire precipitator is used with the same SCA, integrate the grade-efficiency equation to calculate the resulting overall penetration

(a) With no back corona

*Answer: 1.9%*

b) With severe back corona

*Answer: 6.5%*

### 9.16[d]. Multiple cyclone precleaner for an ESP

The gas flow rate through the ESP of Example 9.9 increases to 30 $m^3/s$ because of changes in the capacity of the boiler. Instead of increasing the collection area, the ESP is fitted with a multiple cyclone precleaner with an overall removal efficiency of 80%. The aerosol population leaving the cyclones is log-normally distributed with MMD = 7.0 μm and $\sigma_g = 2.5$. Estimate the overall efficiency of the combined system at the new gas flow rate.

*Answer: 99.6%*

### 9.17[a]. Effect of non-uniform gas velocity on ESP performance

Example 9.9 calculates the overall efficiency of an ESP assuming a uniform gas velocity distribution. If the distribution is characterized by a quality factor of 1.2, estimate the actual efficiency assuming no gas sneakage or reentrainment losses.

*Answer: 99%*

### 9.18[b]. Flow quality factor and statistical measures of velocity nonuniformity

McDonald and Dean (1982) presented the following empirical relationship based on a pilot plant study between $\phi$, the normalized standard deviation of the gas velocity distribution ($\sigma_f$), and the ideal penetration predicted:

$$\phi = 1 + 0.766\left(1 - Pt^{id}\right)\sigma_f^{1.786} + 0.0755\,\sigma_f \ln Pt^{id}$$

where

$$\sigma_f = \frac{\sqrt{\frac{1}{N}\sum_{j=1}^{N}(v_a - v_j)^2}}{v_a}$$

(a) Estimate $\sigma_f$ for the flow distribution conditions of Example 9.10. Estimate the flow quality factor predicted under those conditions by McDonald and Dean's correlation.

*Answer:* $\phi = 1.224$

(b) The ideal overall collection efficiency of an ESP is 99.9% assuming a uniform velocity distribution. If the normalized standard deviation of the actual distribution is 50%, estimate the resulting overall efficiency assuming no losses by gas sneakage or reentrainment.

*Answer: 99%*

### 9.19[c,d]. ESP performance in $SO_2$ dry scrubbing applications

Dry scrubbing processes offer potential cost-effective retrofit FGD technologies for existing coal-fired electric generating stations faced with acid rain legislation. However, the existing particulate control equipment must be capable of collecting both the flyash and the unreacted injected sorbent. The following data were obtained at the TVA 10 MW Spray Dryer/ESP Pilot Plant (Durham et al. 1990):

| Parameter | Baseline Conditions | Spray Dryer Conditions |
|---|---|---|
| Flow rate, $m^3/s$ | 16.35 | 15.5 |
| Temperature, K | 430 | 336 |
| Plate area per section, $m^2$ | 314.4 | 314.4 |
| Number of sections | 4 | 4 |
| Plate spacing, mm | 254 | 254 |
| Average electric field, kV/m | 300 | 370 |
| Inlet size distribution | | |
| MMD, μm | 8.0 | 10.0 |
| $\sigma_g$ | 2.5 | 2.3 |
| Inlet dust concentration, $g/m^3$ | 2.634 | 21.131 |
| Outlet dust concentration, $g/m^3$ | 0.00453 | 0.0355 |

Gas sneakage and the flow quality factor were estimated as 0.05, and 1.1 respectively for both sets of operating conditions. The dielectric constant of the particles for both conditions is about 8.0.

(a) Estimate the reentrainment fraction, *RR*, at baseline conditions.

*Answer: 0.09*

(b) Estimate *RR* at spray dryer conditions

*Answer: 0.158*

(c) Notice that at spray dryer conditions the outlet dust concentration increases significantly as compared to the baseline conditions. Design a new ESP that, at spray dryer conditions, achieves the outlet concentration that characterized baseline conditions. Specify the number of sections and the collection area per section.

### 9.20[b]. Dimensions of an ESP

Specify the dimensions of an ESP to process 50,000 $m^3$/min of a flue gas with 99.5% overall particulate removal efficiency. The effective migration velocity of the particles is 0.1 m/s. Assume that the plate spacing is 400 mm; the aspect ratio is 1.0; and the gas velocity is not to exceed 1.0 m/s. Specify the total collection area, the number of channels, the dimensions of the ESP, and the corona power requirements.

*Answer:* $A_c = 44{,}300\ m^2$

### 9.21[a]. Total capital investment for an ESP

Estimate the TCI and the annual capital recovery cost for the ESP of Problem 9.20. Assume that the cost of auxiliary equipment is $215,000. No special site preparation or buildings are needed. Assume a useful life of 20 yr and no salvage value. The minimum attractive rate of return is 15%/yr.

*Answer: CRC = $2,586,400/yr*

### 9.22[d]. Plate-wire ESP for a Portland cement kiln

In Problem 8.17, a multiple cyclone system was designed as a precleaner for the control of particulate emissions from a Portland cement kiln. For each of the alternatives considered in that problem, design a plate-wire ESP such that the combined system is capable of satisfying the particulate NSPS for the source. The plate spacing must be 400

mm. The dielectric constant of the particles is 6.14; their resistivity is below $10^{11}$ ohm-cm. From scale models, gas sneakage is expected to be about 0.10; rapping reentrainment about 0.10; and the flow quality factor 1.2. For each alternative, specify the following:

(a) Number of sections
(b) Total collection area
(c) TCI and TAC of the combined multiple cyclone-ESP system

Choose between the three alternatives suggested based on the EUAC measure of merit. Assume that the ESP has a useful life of 20 yr with no salvage value. Operating and maintenance labor rates are \$15/h and \$20/h, respectively. The dust collected in both devices can be recycled to the process at no additional cost.